Nuclear Engineering and Design 265 (2013) 599–610

Contents lists available at ScienceDirect

Nuclear Engineering and Design

journal homepage: www.elsevier.com/locate/nucengdes

A 3D transport-based core analysis code for research reactors with unstructured geometry

Tengfei Zhang, Hongchun Wu, Youqi Zheng*, Liangzhi Cao, Yunzhao Li

School of Nuclear Science and Technology, Xi'an Jiaotong University, Xi'an, Shaanxi 710049, China

HIGHLIGHTS

- A core analysis code package based on 3D neutron transport calculation in complex geometry is developed.
- The fine considerations on flux mapping, control rod effects and isotope depletion are modeled.
- The code is proved to be with high accuracy and capable of handling flexible operational cases for research reactors.

ARTICLE INFO

Article history:
Received 27 April 2013
Received in revised form 26 July 2013
Accepted 9 August 2013

ABSTRACT

As an effort to enhance the accuracy in simulating the operations of research reactors, a 3D transport core analysis code system named REFT was developed. HELIOS is employed due to the flexibility of describing complex geometry. A 3D triangular nodal S_N method transport solver, DNTR, endows the package the capability of modeling cores with unstructured geometry assemblies. A series of dedicated methods were introduced to meet the requirements of research reactor simulations. Afterwards, to make it more user friendly, a graphical user interface was also developed for REFT.

In order to validate the developed code system, the calculated results were compared with the experimental results. Both the numerical and experimental results are in close agreement with each other, with the relative errors of k_{eff} being less than 0.5%. Results for depletion calculations were also verified by comparing them with the experimental data and acceptable consistency was observed in results.

© 2013 Elsevier B.V. All rights reserved.

1. Introduction

Progress in industrial nuclear engineering is practically unthinkable without the support by research reactors. Associated with ever increasing demands in terms of safety, quality and economics, the future specific needs are widespread and call for a maximum flexibility and versatility for this kind of facilities. These requirements make the research reactors take on more complicated configurations and irregular assembly geometries, compared with general PWR and BWR. For instance, The "daisy-flower"-shaped layout pattern in France (Döderlein et al., 2008), the plate-pattern fuel assembly configurations (Guillaume and Bruno, 2008; Masao et al., 2008; Salaheddin et al., 2013), and the common hexagonal design concept in Japan (John, 2010), etc. Due to such complex configurations, direct applications of traditional reactor analysis codes are difficult. In order to meet the accuracy requirements associated with the modeling of research reactors, dedicated analysis techniques were developed in the past. For example, the 3D rectangular or hexagonal FEM method by CRONOS2 code was used for JHR simulation (Döderlein et al., 2008). The more prevalent method is the Monte-Carlo method for its advantages in modeling complex geometries (El Bakkari et al., 2010; Salaheddin et al., 2013; Stamatelatos et al., 2007; Shoushtari et al., 2010; Masao et al., 2008; Guillaume and Bruno, 2008). However this method requires prohibitive computational costs when integrated in the reactor core analysis and operational simulations. Such calculations call for high flexibility, which is also a challenge for the Monte-Carlo method. Therefore, the deterministic methods, which have been used extensively in the past for power reactors, highlight their advantages with respect to the higher flexibility, versatility and computational efficiency.

Fig. 1 shows a schematic view of the assemblies and reactor core of a typical research reactor. According to the figure, the reactor core is loaded with assemblies fabricated in complex unstructured geometry, as well as some irregular large exposure channels. The complexity of geometry is a feature that almost all research reactors have and weakens the feasibility of traditional methods using the rectangular or hexagonal meshes. In the research reactors, control rods are frequently operated to adjust the reactivity and realize some special changes. Furthermore, most control rods are in similar

* Corresponding author at: School of Nuclear Science and Technology, Xi'an Jiaotong University, 28 Xianning West Road, Xi'an 710049, China.
Tel.: +86 29 8266 8692; fax: +86 29 8266 8916.
E-mail address: yqzheng@mail.xjtu.edu.cn (Y. Zheng).

0029-5493/$ – see front matter © 2013 Elsevier B.V. All rights reserved.
http://dx.doi.org/10.1016/j.nucengdes.2013.08.068

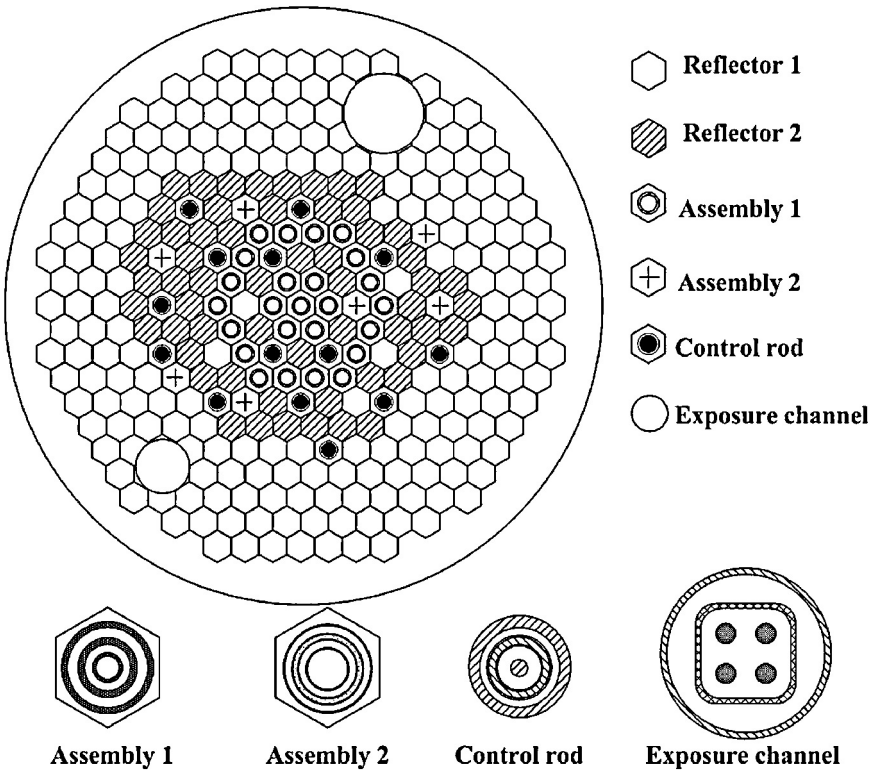

Fig. 1. A schematic view of a typical research reactor core.

size with other assemblies, strong flux variations and heterogeneity arise in the core. Therefore, the 3D whole core transport calculation with fine consideration of the control rods becomes necessary. Combined with the heterogeneous core configuration and small size of the core, the transport calculation becomes very important. Besides, the exposure experiments in the research reactor bring a lot of additional functional requirements to the simulation. These requirements impose many challenges on the core analysis codes currently being used, and emphasize the development of advanced codes with capability of handling calculations with complex geometry, strong heterogeneous effects, possessing high accuracy and flexible functional options.

To meet the requirements, a 3D transport code system for the in-core fuel management calculation for research reactors was developed, with the name of REFT (REsearch reactor Fuel management code system with Transport method). It incorporates the traditional two-step method based on the homogenization theory. The lattice code HELIOS was used to obtain few-group constants (Merk and Koch, 2008; HELIOS, 2009). The 3D neutron transport solver DNTR (Lu, 2007) was employed in the fuel management procedure with the feasibility to handle complex geometric modeling.

Considering the possible characteristics of research reactors, this work establishes applicable models for the fuel management calculation. The functions for criticality searching, flux distribution reconstruction and micro-depletion calculation were employed in the code system. A front-end system providing look-and-feel graphical user interface and a comprehensive tool set for automation was also developed. This system also provides the platform for visual evaluation of the computational results.

2. Calculation model

2.1. Flow scheme and function overview

The flow chart of the implemented code system is shown in Fig. 2. HELIOS is a powerful lattice code capable of dealing

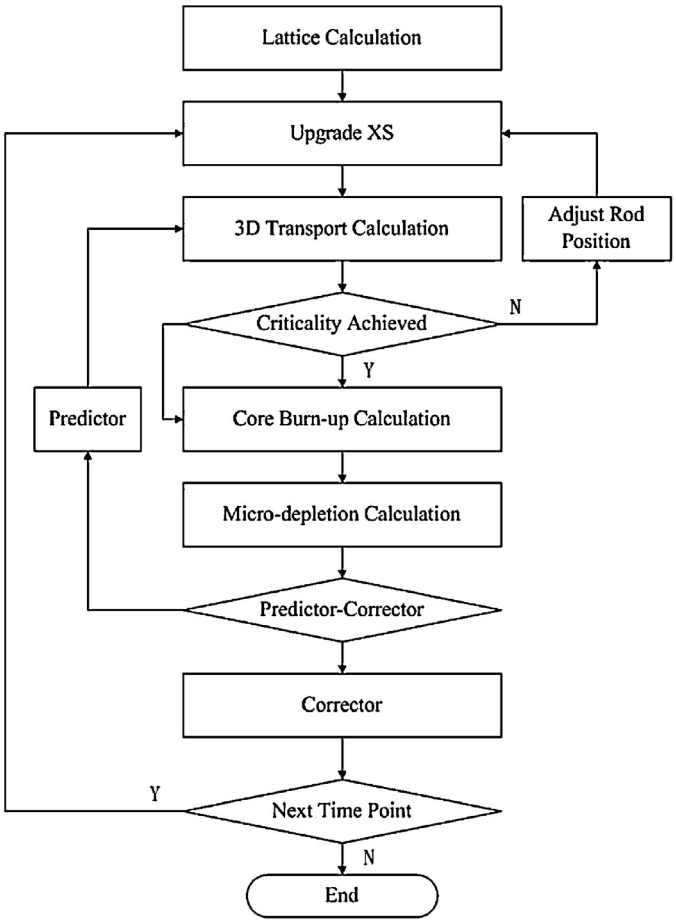

Fig. 2. Flow scheme of REFT.

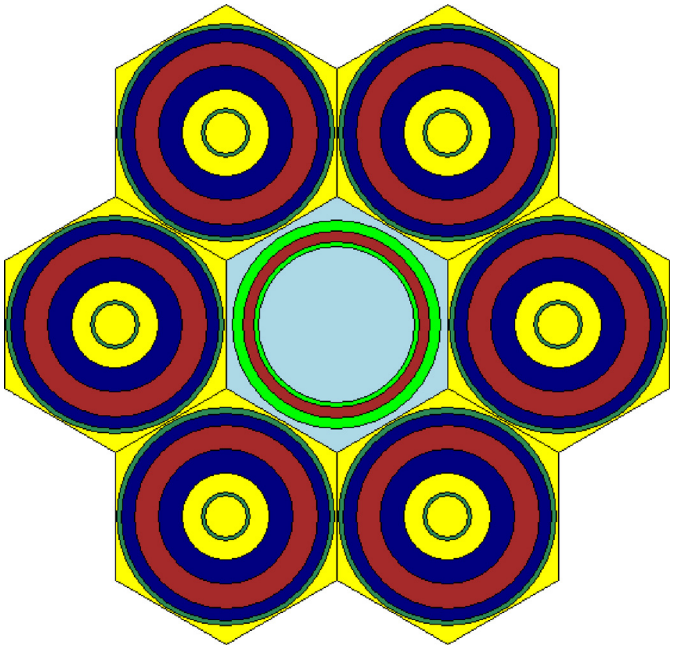

Fig. 3. Schematic view of the super assembly model.

with almost any type of 2-D geometry. The assembly is modeled using HELIOS, and few-group constants are generated and fitted in polynomials. During the in-core fuel management calculation, the variation of states can be predicted for a series of time steps, so as to simulate the whole operation history of a reactor (Li et al., 2010). In-core transport calculation is performed by the 3D neutron transport solver DNTR, which is capable of handling complex unstructured geometry (Lu, 2007). To compensate for excess reactivity, the adjustment of control rod position is taken into account and a dedicated technique is utilized to mitigate the cusping effect. For the special requirements such as isotope production and radiation tests, the fine depletion calculation involving micro-depletion and the predictor-corrector method are used.

2.2. Few group constants calculation

The traditional two-step method can be separated as: firstly calculate the few-group homogenized cross sections of different assemblies under different states. Secondly, perform the 3D core analysis using the cross sections.

HELIOS is a two-dimensional lattice code, using energy-group nuclear data library from the ENDF-B/VI. The subgroup method is used to perform the resonance calculation. The transport method involved is the current-coupling collision probability (CCCP) method (HELIOS, 2009).

The accuracy of few-group cross section is the prerequisite for successful whole core simulations. HELIOS allows for direct geometry applications with the least degree of simplification. A schematic view for the super-assembly control rod model is shown in Fig. 3. Modeling the assemblies in their most exquisite geometry, the accuracy of few-group cross section is guaranteed to a higher level. In HELIOS, the assembly to be calculated consists of space elements that are coupled by interface currents. Transport calculations are performed with CP method inside each space element, and then the space elements are coupled with each other and with the boundaries by interface currents. High order interface coupling will need large storage memory and computational time, so a coupling order of 2 is chosen where possible. To perform lattice calculations, the reflective boundary condition is imposed on each side of the geometry. A special buckling is searched to consider the effect of leakage in calculating the neutron spectrum in lattices. The neutron spectrum in multi-group form is corrected by the leakage model before it is applied to collapse the few group cross sections. Considering the fact that all the critical facilities have similar geometry and material composition with the research reactor, once the buckling has been specified, it is fixed for all critical facilities and the research reactor.

During the depletion calculation process, the constants are seen as polynomials with respect to the burn-up and the relative power (or the fuel temperature). The boric concentration is taken into account for the functional extension, since it may be used to suppress excess reactivity sometimes. The cross sections are fitted into the following form:

$$\Sigma_X = f_1(B_U, C_B) f_2(P_r)$$

where f_1, f_2 are polynomials of their respective variables; B_U is the burn-up value (MWd/tU); C_B is the boric concentration (ppm); and P_r is the relative power. Note that the influence of ^{135}Xe and ^{149}Sm in terms of local absorption cross-section is significant, the contribution is eliminated in the fitting process. Instead, micro depletion calculation is used to estimate their specific contributions in the depletion process.

2.3. In-core neutron transport calculation

The unstructured assembly patterns in research reactors call for flexible modeling techniques. The strong heterogeneity makes the diffusion method not applicable to meet the requirements in accuracy. Thanks to the powerful geometric modeling capability, the three-dimensional neutron transport solver DNTR based on the triangular meshes is adopted in REFT.

In DNTR, the calculations are based on the S_N nodal method in triangle-z meshes. Unlike the rectangular or hexagonal meshes, the triangular meshes are not the same in the shapes and sizes. Here the transverse integration procedure cannot be applied simply as in most nodal methods. To solve the node transport equations, the triangular meshes are transformed into equilateral ones using the area coordinates. The method can be expressed as follows (Lu, 2007).

Suppose P is a point inside an arbitrary triangle, and divide the triangle into three triangles by connecting P with three vertexes. The areas of these four triangles are Δ, Δ_1, Δ_2, Δ_3, respectively. Then the area coordinates of the point P can be defined as:

$$\lambda_1 = \frac{\Delta_1}{\Delta}, \quad \lambda_2 = \frac{\Delta_2}{\Delta}, \quad \lambda_3 = \frac{\Delta_3}{\Delta}$$

Thus the relationship between the orient physical coordinate and the area coordinate is established. Using this relationship twice, the arbitrary triangles in physical coordinate (x, y) can be transformed to the ones in area coordinate $(\lambda_1, \lambda_2, \lambda_3)$ and then transform them to the regular ones in the coordinate (x', y'), as is seen in Fig. 4.

The final expression can be written as:

$$x = \frac{x_1 + x_2 + x_3}{3} + \left(-x_1 + \frac{x_2 + x_3}{2}\right) x' + \frac{\sqrt{3}(-x_2 + x_3)}{2} y'$$

$$y = \frac{y_1 + y_2 + y_3}{3} + \left(-y_1 + \frac{y_2 + y_3}{2}\right) x' + \frac{\sqrt{3}(-y_2 + y_3)}{2} y'$$

where $x_1, x_2, x_3, y_1, y_2, y_3$ are the coordinates of three vertexes.

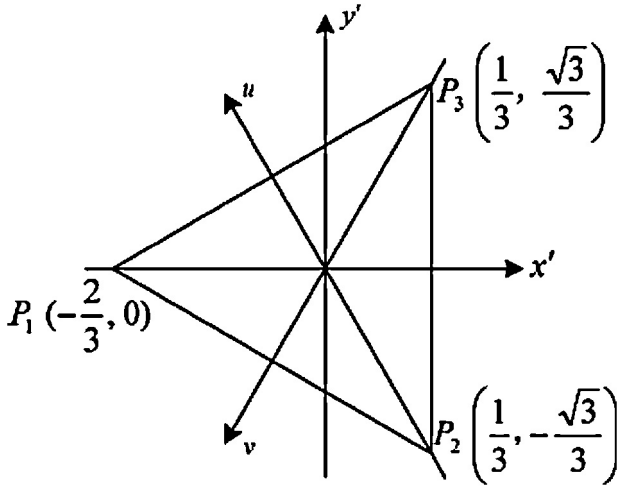

Fig. 4. Equilateral triangle mesh.

The neutron transport equation written in standard notation can be expressed as:

$$\mu^m \frac{\partial \phi^m(x,y,z)}{\partial x} + \eta^m \frac{\partial \phi^m(x,y,z)}{\partial y} + \frac{\xi^m}{h_z} \frac{\partial \phi^m(x,y,z)}{\partial z} + \sum\nolimits_t \phi^m(x,y,z) = Q(x,y,z) \quad (1)$$

where h_z is the nodal axial width and m stands for the discrete direction. The values μ^m, η^m and ξ^m are the cosines of angular variables relative to x, y and z directions axis. Using the coordinate transformation, we obtain the equation as:

$$\mu_x^m \frac{\partial \phi^m(x',y',z')}{\partial x'} + \eta_x^m \frac{\partial \phi^m(x',y',z')}{\partial y'} + \frac{\xi^m}{h_z} \frac{\partial \phi^m(x',y',z')}{\partial z'} + \sum\nolimits_t \phi^m(x',y',z) = Q(x',y',z) \quad (2)$$

where:

$$\mu_x^m = \frac{(-y_2+y_3)\mu^m + (x_2-x_3)\eta^m}{2\Delta}$$

$$\eta_x^m = \frac{(-x_1+(1/2)x_2+(1/2)x_3)\eta^m + (y_1-(1/2)y_2-(1/2)x_3)\mu^m}{\sqrt{3}\Delta}$$

$$-\frac{2}{3} \le x \le x \le \frac{1}{3}, \quad -y_s(x) \le y \le y_s(x), \quad y_s(x) = \frac{x+(2/3)}{\sqrt{3}}$$

The nodal balance equation is given by:

$$2\mu_x^m \bar{\phi}_x^m + 2\eta_u^m \bar{\phi}_u^m + 2\mu_v^m \bar{\phi}_v^m + \frac{\xi^m}{h_z}(\bar{\phi}_{z+}^m - \bar{\phi}_{z-}^m) + \Sigma_t \bar{\phi}^m = \bar{Q} \quad (3)$$

$\bar{\phi}_i^m (i = x, u, v)$ is the averaged outgoing surface flux in the x, u, v directions, as is shown in Fig. 4; $\bar{\phi}_{z\pm}^m$ are the outgoing surface averaged flux of the upper and lower sides of the node; $\bar{\phi}^m$ is the averaged flux in the node. With dedicated sweeping and source iteration method, the transport calculation is accomplished.

2.4. Control rod cusping effect

The axial movements of control rods are incorporated in some research reactors to compensate for the excess reactivity or some other variations. The differential worth of control rod is very important for the whole-core simulation. The node which is partly inserted by the control rod can be separated in two parts: the rodded section and the unrodded section. The rodded section is the part occupied by control rod absorption material, while the unrodded section is occupied by other kind of material. Nodal methods model control rod motions as spatially uniform changes in the macroscopic cross sections. When simulating the control rod differential worth, a simple volume-weighted average of the rodded and unrodded nodal cross sections may induce a cusp-like behavior because of the fact that the neutron flux within the node is not spatially flat (Jess, 1992). Therefore, an elaborate correction scheme is incorporated in REFT. The method can be illustrated as follows.

Assume the kth node in the axial direction is partly inserted by a control rod. Define the rodded section of the node as S_R and the unrodded one as S_{NR} (Yamamoto, 2004). In this node, the averaged flux of S_R and S_{NR} can be approximated by:

$$\phi_{S_{NR},g} = \frac{\Delta z_{k-1}\phi_{k-1,g} + (1-f_R)\Delta z_k \phi_{k,g}}{\Delta z_{k-1} + (1-f_R)\Delta z_k} \quad (4)$$

$$\phi_{S_R,g} = \frac{\Delta z_{k+1}\phi_{k+1,g} + f_R \Delta z_k \phi_{k,g}}{\Delta z_{k+1} + f_R \Delta z_k} \quad (5)$$

where $\phi_{S_{NR},g}$ and $\phi_{S_R,g}$ are the averaged flux of the two sections; Δz_{k-1}, Δz_k, Δz_{k+1} are the height of the $(k-1)$th, kth and $(k+1)$th node (cm); f_R is the ratio of S_R to that of the kth node. Based on the approximation, the modified cross sections of the kth node can be written as:

$$\bar{\Sigma}_{x,g} = \frac{(1-f_R)\Sigma_{S_{NR},x,g}\phi_{S_{NR},g} + f_R \Sigma_{S_R,x,g}\phi_{S_R,g}}{f_R\phi_{S_R,g} + (1-f_R)\phi_{S_{NR},g}} \quad (6)$$

In Eq. (6), $\Sigma_{S_{NR},x,g}$ and $\Sigma_{S_R,x,g}$ are the cross sections of the unrodded and rodded section of the node, respectively. With the modified cross sections, the transport calculation is performed again to give a better estimation of the control rod differential worth.

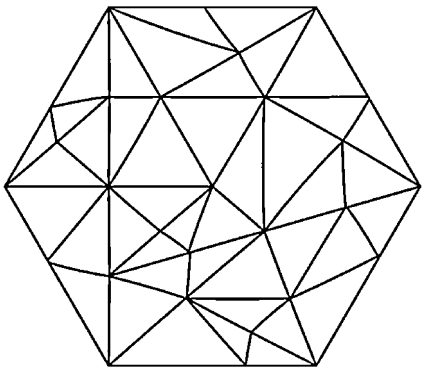

Fig. 5. Mesh for a hexagonal assembly.

2.5. Depletion calculation

2.5.1. Flux distribution reconstruction

By the nodal method, only the averaged flux inside each node can be obtained. In research reactors, special requirements such as the ones from exposure tests and isotope production, call for knowledge of more specific flux distribution inside each assembly. These necessities the flux distribution reconstruction scheme in REFT. To resolve this issue, we take advantage of the triangular nodal method.

Take the hexagonal assembly as an example. In the triangular nodal method, it will be meshed into several triangles, seen in Fig. 5. Assume the number of triangular nodes inside the assembly as N, the coordinates of their gravity centers are (x_i, y_i), $i = 1, N$. The averaged flux of node i is $\bar{\phi}_i$, which can be calculated by the transport solver, is regarded as equal to the flux value at its gravity center.

Expand the flux distribution inside the assembly in the following form:

$$\phi(x,y)=\sum_{\substack{p=0\\q=0}}^{m,n} a_{p,q}x^p y^q \tag{7}$$

where $a_{p,q}$ is the coefficient of each expansion and m, n are the highest expansion orders of x and y, respectively. In order to get the value of the expansion coefficient $a_{p,q}$, recall the least square method, define the variance as:

$$F=\sum_{i=1}^{N}(\phi(x_i,y_i)-\bar{\phi}_i)^2 \tag{8}$$

Substitute Eq. (7) into Eq. (8) we obtain:

$$F=\sum_{i=1}^{N}(a_{p,q}x_i^p y_i^q-\bar{\phi}_i)^2 \tag{9}$$

Eq. (9) can be further expanded to:

$$F=\sum_{i=1}^{N}\left(\sum_{\substack{p=0\\q=0}}^{m,n} a_{p,q}^2 x_i^{2p}y_i^{2q}+\bar{\phi}_i^2-2\bar{\phi}_i x_i^p y_i^q+2\sum_{\substack{p'=0\\q'=0\\p'\neq p\\q'\neq q}}^{m,n} a_{p',q'}x_i^{p+p'}y_i^{q+q'}\right) \tag{10}$$

Calculate each partial derivative of $a_{p,q}$ and the simplification can be defined as:

$$\frac{\partial F}{\partial a_{p,q}}=\sum_{i=1}^{N}\left(2\sum_{\substack{p'=0\\q'=0}}^{m,n} a_{p',q'}x_i^{p+p'}y_i^{q+q'}-2\bar{\phi}_i x_i^p y_i^q\right) \tag{11}$$

This system is put into a matrix notation as:

$$\boldsymbol{Ax}=\boldsymbol{B} \tag{12}$$

where $\boldsymbol{A}$ is a M×M matrix, $\boldsymbol{x}$ and $\boldsymbol{B}$ are vectors whose dimensions equal M, with $M=(m+1)(n+1)$.

Elements of matrix $\boldsymbol{A}$ can be written as:

$$A_{p+q,p'+q'}=\sum_{i=1}^{N}x_i^{p+p'}y_i^{q+q'} \tag{13}$$

The indices of rows are dominated by variables p and q, where p is from 0 to m and varies fastest, then q varies from 0 to n; the indices of columns are controlled by variables p' and q', where p' is from 0 to m and varies fastest, then q' varies from 0 to n. Then vector $\boldsymbol{x}$ can be written as:

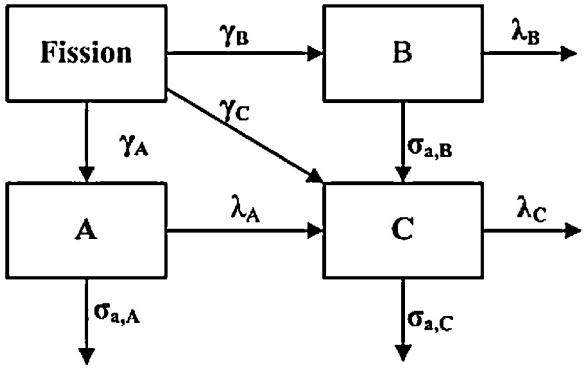

Fig. 6. Simplified isotopic depletion scheme.

$$\boldsymbol{x}=col\{a_{0,0},\ a_{0,1},\ a_{0,2}\ \ldots\ a_{0,n},\ a_{1,0},\ a_{1,1}\ \ldots\ a_{m,n}\} \tag{14}$$

and elements of vector $\boldsymbol{B}$ are denoted in the form:

$$B_{p+q}=\sum_{i=1}^{N}x_i^p y_i^q\bar{\phi}_i \tag{15}$$

The indices of rows are controlled by variables p and q, where p is from 0 to m and varies fastest. q is from 0 to n, varies second.

The matrix can be solved easily by the methods such as the Gauss–Seidel iteration. Then we obtain the expression of the spatial flux distribution expressed in Eq. (7).

Using $\phi(x,y)$ in Eq. (7) we could conveniently evaluate the flux inside specified region in assemblies:

$$\bar{\phi}_V=\frac{\iint_V\phi(x,y)dV}{\iint_V dV} \tag{16}$$

where V is the specified region. Imposing the form factor of heterogeneous calculation by HELIOS, the actual flux inside the region can be recovered wherever needed.

2.5.2. Micro-depletion model

In research reactors, the changes of nuclide density in the targets should be treated more accurately than those of other regions. The micro-depletion method allows for advanced capabilities particularly applying for depletion simulations in the research reactor.

The depletion scheme of isotopes can be approximately described by Fig. 6. The depletion equations with respect to isotopes A, B and C can be written in the following form:

$$\begin{cases}\dfrac{dN_A(t)}{dt}=F_A-L_A N_A(t)\\ \dfrac{dN_B(t)}{dt}=F_B-L_B N_B(t)\\ \dfrac{dN_C(t)}{dt}=F_C+\lambda_A N_A(t)+A_B N_B(t)-L_C N_C(t)\end{cases} \tag{17}$$

where N_X is the number density of isotope X (A, B, C) (cm^{-3}); F_X is the fission production rate of isotope X ($s^{-1}\,cm^{-3}$); $L_X=\lambda_X+\sigma_{a,X}\phi$ is the decreasing rate of isotope X (s^{-1}); A_X is the absorption rate of isotope X(s^{-1}); λ_X is the decay constant of isotope X (s^{-1}).

Under the premise of initially given nuclide densities and after a series of derivations, the solutions can be written as:

$$\begin{cases} N_A(t) = N_A(0)e^{-L_A t} + \dfrac{F_A}{L_A}(1 - e^{-L_A t}) \\ N_B(t) = N_B(0)e^{-L_B t} + \dfrac{F_B}{L_B}(1 - e^{-L_B t}) \\ N_C(t) = \dfrac{F_C + (F_B A_B/L_B) + (F_A\lambda_A/L_A)}{L_C} + \dfrac{N_A(0)\lambda_A - (F_A\lambda_A/L_A)}{L_C - L_A}e^{-L_A t} + \dfrac{N_B(0)A_B - (F_B A_B/L_B)}{L_C - L_B}e^{-L_B t} \\ + \left[\left(N_C(0) - \dfrac{F_C + (F_B A_B/L_B) + (F_A\lambda_A/L_A)}{L_C} + \dfrac{N_A(0)\lambda_A - (F_A\lambda_A/L_A)}{L_C - L_A} + \dfrac{N_B(0)A_B - (F_B A_B/L_B)}{L_C - L_B}\right)e^{-L_C t}\right] \end{cases} \quad (18)$$

The number density of specified isotope at each burn-up step can be updated once the flux in the depletion region is obtained. Using the flux reconstructed in Eq. (16) and by substitution of the actual flux density into Eq. (18), the number density of isotopes can be obtained. The cross-sections of the node containing the isotope are then flux-volume weighted.

2.5.3. Predictor–corrector process

The predictor–corrector method is incorporated in REFT to enhance the accuracy of depletion calculation scheme (HELIOS, 2009). The procedure is illustrated in Fig. 7.

The depletion process from burn-up E_1 to burn-up E_2 assumes the flux to be constant and equal to ϕ_1 at E_1, whereas actually the flux varies all the time. With the new isotopic number densities thus found, $N_2(\phi_1)$, the flux ϕ_2 at burn-up level E_2 is calculated. This corresponds to the upper part of Fig. 7 where it is called the predictor step.

Often, the next burn-up step is made with a constant ϕ_2, and with $N_2(\phi_1)$as the initial number densities, and so on. To guarantee the accuracy, very small burn-up steps are needed to justify the assumption of constant flux in the steps. To enhance the efficiency, the depletion calculation from E_1 to E_2 is done with some sort of averaged flux. Referring to Fig. 7, the depletion calculation from E_1 to E_2 is done a second time with the loss and gain rates pertinent to ϕ_2. This is the corrector step shown in the lower part of Fig. 7. It produces the number densities $N_2(\phi_2)$. The final number densities at E_2 are then obtained as the average of $N_2(\phi_1)$ and $N_2(\phi_2)$.

2.6. The graphical user interface

The graphical user interface REFT-INT is developed to facilitate the input preparation process and make the output information straightforward. The function of the interface can be illustrated as follows:

(1) Shoulder the burdens of editing tedious input cards. For instants, generating controlling parameters such as the order of S_N methods, iteration convergence criteria, geometry information of the core. Users can conveniently model the whole-core assembly configuration without knowing much about input rules. See Fig. 8.
(2) Dump the assembly information for future restart calculations. An element database is set up to save the information.
(3) Invoke the execution of REFT as a black box.
(4) Read output parameters to show maps of relative power, flux, burn-up distributions, as well as their respective axial distributions, differential control rod worth curves, etc.

Fig. 9 shows the work flow of REFT-INT, where the blue blocks represent the internal coupling between REFT-INT modules.

3. Numerical results

The models described above have been integrated into REFT. This code was verified against several numerical tests, including a PWR fuel pin problem, the KNK benchmark and a series of experimental tests. The continuous-energy Monte Carlo results are also listed as the references where available.

Results showed that higher order angular discretizations provide only limited accuracy improvements but call for much larger storage memory and computation time, so all of the results are evaluated with the angular discretization order of S_4. The triangular node meshing is automatically performed by ANSYS. Both REFT and the continuous-energy Monte Carlo calculations are performed using PC with 3.40 GHz Intel i7-2600 CPU processor.

3.1. The PWR fuel pin problem

In this case, a burn-up simulation of PWR fuel pin is performed by REFT to give preliminary verifications. The result of HELIOS is employed as the reference. Geometry parameters are exemplified in Fig. 10. The reflective boundary condition and zero axial buckling are assumed. Table 1 shows detailed material parameters of the fuel pin.

By using HELIOS, the 4-group cross sections are collapsed and then the depletion process is recovered by using REFT based on the 4-group cross sections. The direct calculation by using HELIOS is performed to give the reference results. The final comparison presented in Fig. 11 shows a maximum k_{eff} discrepancy of 0.272%.

3.2. The KNK benchmark

This benchmark calculates a core with the vacuum boundary conditions, which has the hexagonal-z geometry as shown in Fig. 12 (Lu, 2007).

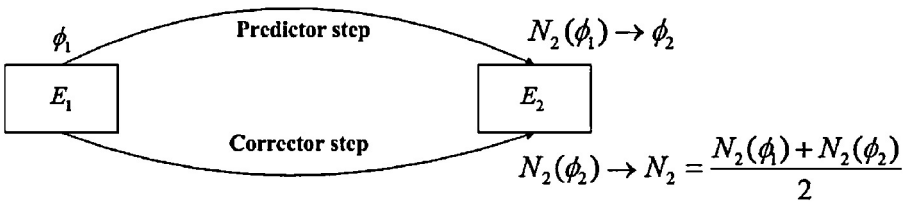

Fig. 7. Predictor–corrector method.

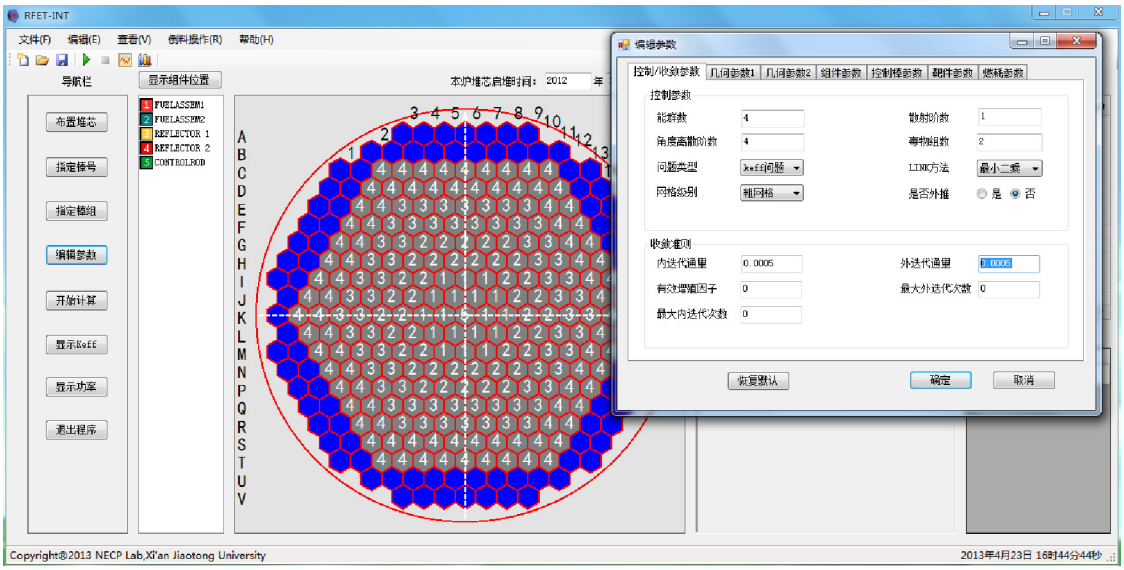

Fig. 8. Input process using REFT.

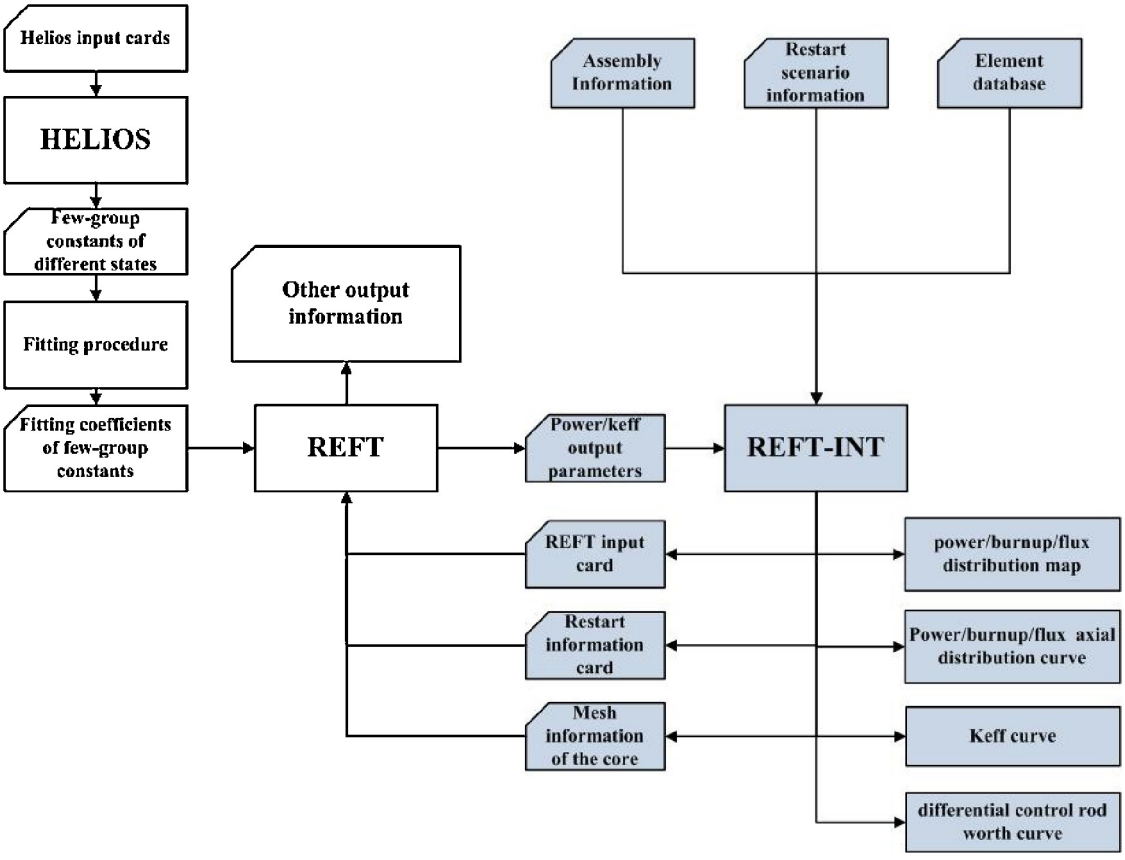

Fig. 9. Flow scheme of the REFT interface.

Table 1
Atomic number densities of materials in the fuel pin.

Material	Number densities/10^{24}/cm^3					
	^{235}U	^{238}U	^{16}O	^{16}O	^{1}H	Zr
Fuel (UO_2)	0.00115467	0.02193873	0.0461868	–	–	–
Cladding	–	–	–	–	–	0.04360
Moderator	–	–	–	0.03362	0.06723	–

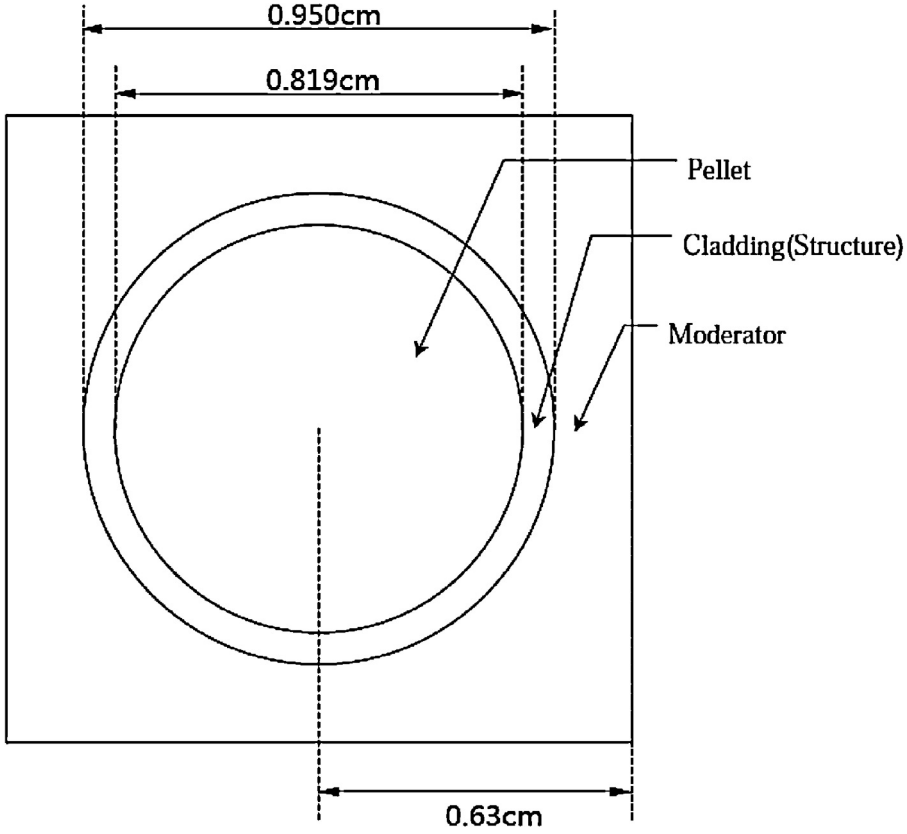

Fig. 10. Schematic view of the fuel pin.

Three cases pertinent to the core were carried out:

Case1: Control rods withdrawn.
Case2: Control rods half inserted.
Case3: Control rods fully inserted.

All cases were performed with the actual configuration meshed in 1914×27 nodes. The reference value is given by the Monte-Carlo calculation code GMVP (Sugino and Takeda, 1996). Table 2 shows the k_{eff} discrepancy estimations. The results of eigenvalues from REFT agree well with those from the Monte-Carlo calculation with the differences being less than 0.1%. Table 3 shows the differences in region averaged group-wise flux for the rod-half-inserted case. The maximum relative error is less than 1%.

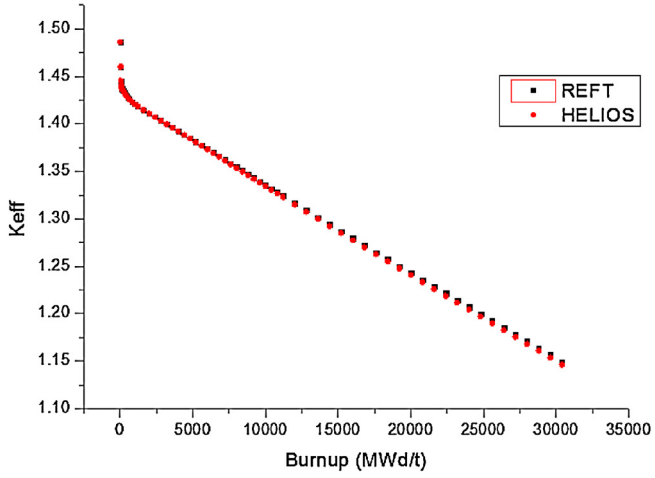

Fig. 11. Comparison of k_{eff}.

Table 2
Comparisons of k_{eff} for KNK benchmark.

	GMVP	REFT	Error (%)
Case 1	1.0955 ± 0.0005[a]	1.0961	0.06
Case 2	0.9839 ± 0.0004	0.9846	0.07
Case 3	0.8802 ± 0.0004	0.8810	0.09

[a] Relative standard deviation.

3.3. The critical facilities problem

Four critical facilities numbered from 1# to 4# are given for tests. The loading configurations are shown in Fig. 13. Two types of reflectors are deployed. The thickness of axial reflector is 16 cm except that of 4#, which is 20 cm. In order to make the comparison more rigorous, the calculations using the continuous-energy Monte Carlo method were performed. The results from experiments were chosen as references. The execution time of REFT was also compared with the continuous-energy Monte Carlo method. The k_{eff} results in Table 4 show that numerical results agree well with references with a maximum error of about 0.3%. It is also significant that by using REFT, the computation time is about 1/35–1/50 of that used by the continuous-energy Monte Carlo method, with hardly any compromise in accuracy.

3.4. The reactor core problem

In this case, a research reactor was modeled to demonstrate the feasibility of REFT. The schematic loading pattern of the reactor is presented in Fig. 1.

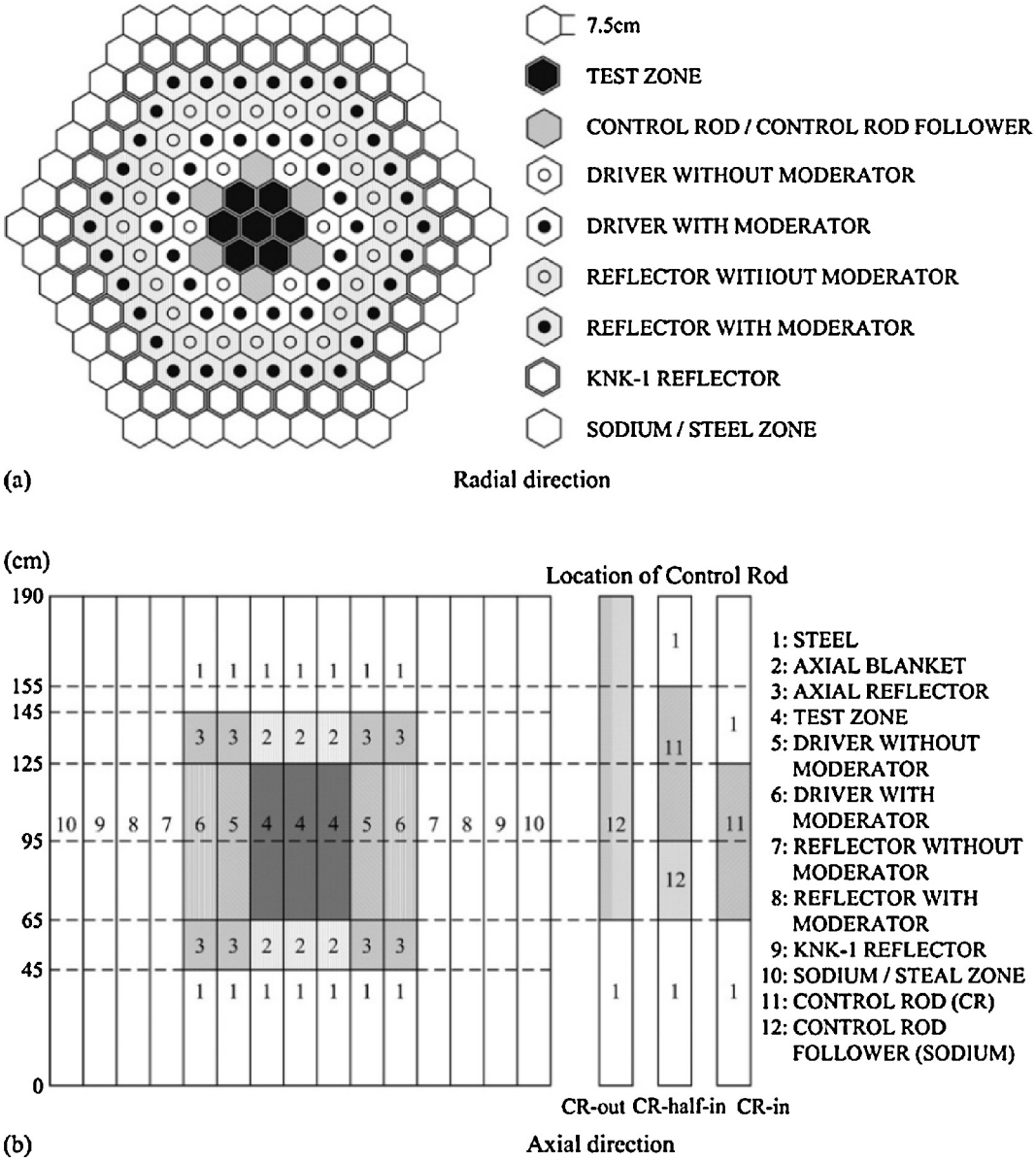

Fig. 12. Core configuration of KNK benchmark.

3.4.1. The CZP of the core

During the operational process, the movements of control rods are used to compensate for the excess reactivity. REFT is used to simulate the critical position of control rod in the cold-state zero power condition.

Taking the experimental result as the reference, the result of REFT is consistent with the reference with the k_{eff} discrepancy tabulated in Table 5 being less than 0.3%. The schematic distribution in Fig. 14 shows the differences of flux between numerical results and experimental ones. Comparisons present acceptable relative errors less than 8% in most assemblies. For the reason that the experiment was carried out from the distant past, the maximum error of −16.22% is supposed to be caused by measuring error in the experiments.

Table 6 gives the comparison of axial heterogeneous factors of several typical assemblies. The maximum relative error which is less than 3% can meet the requirements of engineering analysis.

3.4.2. The operational cycle of the core

REFT was imposed on the operational cycle simulation of the research reactor in terms of depletion analysis and control rod movement prediction. In this case the experimental parameters were chosen as references to give the highest reliability. The loading pattern of the reactor is the same as shown in Fig. 1. REFT simulates the reactor with the initially given positions of control rods, and the good agreement of 0.43% k_{eff} difference is achieved.

Then the whole cycle scheme of a disposal burn-up of 1100 MW d was simulated. In this performance the control rod positions were set at initial height of 0 cm at the beginning of cycle, and a process of criticality searching and depletion calculation is implemented. Control rod positions at the end of the cycle are compared between the numerical estimation and the experimental results. In order to make the discrepancy obvious, in this simulation we set all the control rod bundle positions consistent with the reference, except the last one. This means all the errors will be accumulated to the last bundle. The numerical height of the last bundle

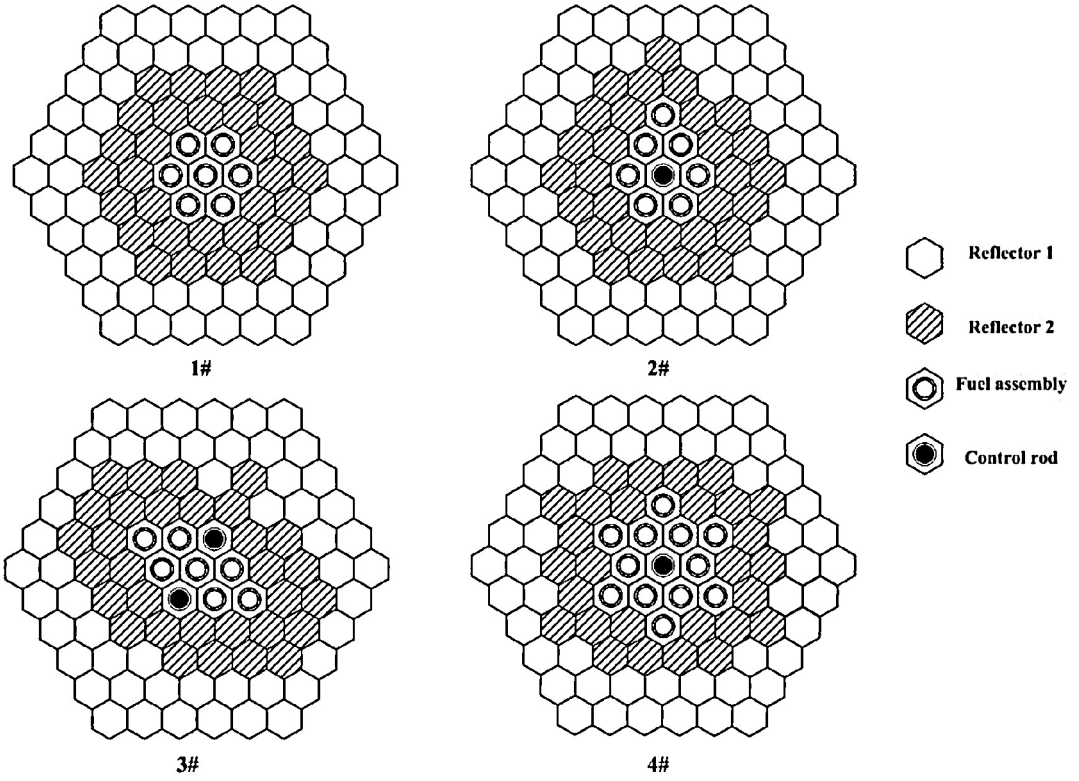

Fig. 13. Loading configurations of critical facilities.

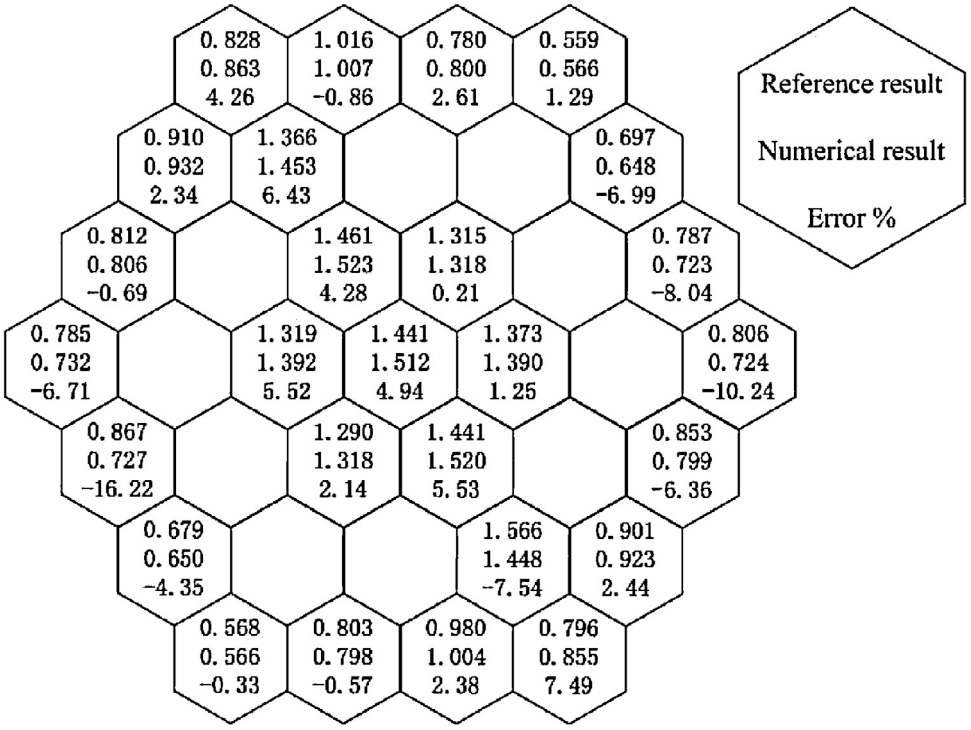

Fig. 14. Flux distribution.

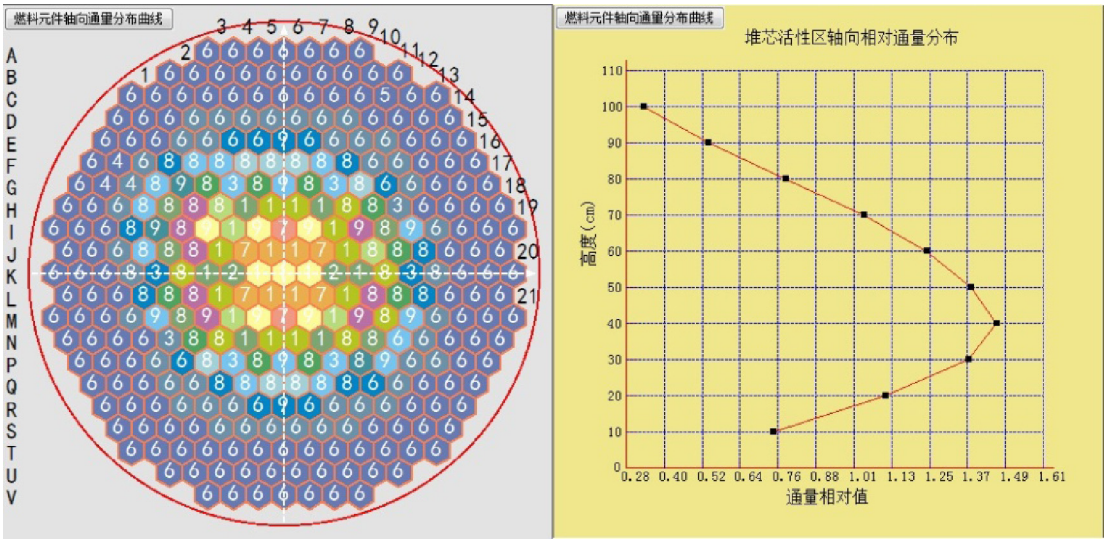

Fig. 15. Averaged radial and axial relative flux distributions at the end of the cycle.

Table 3
Normalized region averaged group fluxes and differences for KNK benchmark.

	GMVP		Error (%)
Axial blanket			
1G	3.183E−01	3.171E−01	−0.38
2G	4.164E−01	4.161E−01	−0.09
3G	1.910E−01	1.921E−01	0.57
4G	7.425E−02	7.472E−02	0.64
Test zone			
1G	5.141E−01	5.126E−01	−0.29
2G	3.864E−01	3.878E−01	0.36
3G	9.108E−02	9.113E−02	0.06
4G	8.453E−03	8.500E−03	0.56
Driver without moderator			
1G	4.876E−01	4.882E−01	0.13
2G	3.687E−01	3.682E−01	−0.14
3G	1.189E−01	1.188E−01	−0.03
4G	2.484E−02	2.476E−02	−0.32
Control rod			
1G	5.025E−01	5.039E−01	0.28
2G	4.038E−01	4.021E−01	−0.43
3G	8.689E−02	8.731E−02	0.49
4G	6.795E−03	6.741E−03	−0.79
Control rod follower			
1G	4.459E−01	4.433E−01	−0.58
2G	3.747E−01	3.760E−01	0.35
3G	1.383E−01	1.394E−01	0.79
4G	4.121E−02	4.136E−02	0.35

is 85.3 cm and the reference height is 88.8 cm. This 3.5 cm height difference is estimated as a reactivity discrepancy of 146 pcm. The evaluation confirms the correct implementation of the methods as well as the performance of the code.

Table 5
k_{eff} relative error of the first core loading pattern.

REFT	Reference	Error
0.9972	1.0000	0.28%

Table 6
Comparison of axial heterogeneous factors of typical assemblies.

Assembly No.	Numerical result	References	Error %
1	1.390	1.382	0.608
2	1.386	1.353	2.496
3	1.390	1.372	1.341

The averaged radial and axial relative flux distributions generated by the interface at the end of the cycle are presented in Fig. 15.

4. Conclusion

Aiming at enhancing the accuracy in the analysis of research reactors, this paper describes a new in-core fuel management calculation code system REFT. In the system, HELIOS was employed to perform the lattice calculation for its flexibility in describing complex geometry. The triangular nodal S_N transport solver DNTR was used to enhance the accuracy of core analysis, overcoming the difficulties from small reactor size and strong heterogeneity. The methods of flux distribution reconstruction, micro-depletion calculation and predictor–corrector depletion evaluation as well as techniques to mitigate control rod cusping effect were incorporated in the code system. At the same time, a front-end of the system providing look-and-feel graphical user interface was also developed.

Table 4
Comparison of k_{eff} between REFT, Monte Carlo method and references.

	REFT			Monte Carlo			References
	k_{eff}	Error	CPU time (min)	k_{eff}	Error	CPU time (min)	
1#	1.0027	0.27%	4.16	1.0006 ± 0.0002[a]	0.06%	202.24	1.0000
2#	1.0004	0.04%	4.65	1.0009 ± 0.0002	0.09%	202.12	1.0000
3#	0.9969	0.31%	4.29	0.9974 ± 0.0002	0.26%	200.39	1.0000
4#	1.0010	0.10%	4.89	0.9987 ± 0.0002	0.13%	178.48	1.0000

[a] Relative standard deviation.

Numerical results show that the average error of reactivity evaluation is small enough compared with the references. Excellent consistency with both numerical and experimental references was observed in the depletion calculation. Flux estimations also possess acceptable accuracy. All the results prove that the new code system can be well used in the core analysis and in-core fuel management simulation of reactors with complex geometry. Interfaces for future upgrade are preserved. The further work is to validate it more by using new experimental data.

Acknowledgements

This work is supported by the National Natural Science Foundation of China (Approved number Nos. 11105104 and 91226106). The authors would like to acknowledge Charles A. Wemple for the fruitful discussions regarding the use of HELIOS.

References

Döderlein, C., et al., 2008. The 3D neutronics scheme for the development of the Jules-Horowitz-reactor. In: International Conference on the Physics of Reactors Nuclear Power: A Sustainable Resource, Casino-Kursaal Conference Center, Interlaken, Switzerland, September 14–19, 2008.

Bakkari El, B., et al., 2010. Monte Carlo modelling of TRIGA research reactor. Rad. Phys. Chem. 79 (2010), 1022–1030.

Guillaume, C., Bruno, D., 2008. HFR advanced computation's models. In: International Conference on the Physics of Reactors Nuclear Power: A Sustainable Resource, Casino-Kursaal Conference Center, Interlaken, Switzerland, September 14–19, 2008.

HELIOS, 2009. Methods. Studsvik Scandpower.

Jess, C.G., 1992. A Quasi-static Polynomial Nodal Method for Nuclear Reactor Analysis. Department of Nuclear Engineering, MIT, Cambridge, MA, USA (Ph.D. Thesis).

John, D.B., 2010. Benchmark evaluation of the start-up core reactor physics measurements of the High Temperature Engineering Test Reactor. In: PHYSOR 2010 – Advances in Reactor Physics to Power the Nuclear Renaissance, Pittsburgh, Pennsylvania, USA, May 9–14, 2010.

Li, Y., Wu, H., et al., 2010. FMSR: a code system for in-core fuel management calculation of aqueous homogeneous solution reactor. Nucl. Eng. Des. 240, 763–770.

Lu, H., 2007. A nodal S_N transport method for three-dimensional triangular-z geometry. Nucl. Eng. Des. 237, 830–839.

Masao, K., et al., 2008. Full core burn-up calculation at JRR-3 with MVP-BURN. In: International Conference on the Physics of Reactors Nuclear Power: A Sustainable Resource, Casino-Kursaal Conference Center, Interlaken, Switzerland, September 14–19, 2008.

Merk, B., Koch, R., 2008. On the influence of spatial discretization in LWR cell- and lattice calculations with HELIOS 1.9. Ann. Nucl. Energy 35 (2008), 1492–1501.

Salaheddin, R.M., et al., 2013. Prediction of neutron energy spectrum in a typical MTR type research reactor using Monte Carlo simulations. Ann. Nucl. Energy 56, 17–22.

Shoushtari, M.K., et al., 2010. Monte Carlo simulation of a research reactor with nominal power of 7 MW to design new control safety rods. Nucl. Instrum. Methods Phys. Res. B 268, 519–523.

Stamatelatos, I.E., et al., 2007. Monte Carlo simulation of the Greek Research Reactor neutron irradiation facilities. Nucl. Instrum. Methods Phys. Res. B 263, 136–139.

Sugino, K., Takeda, T., 1996. An improvement of the transverse leakage treatment for the nodal S_N transport calculation method in hexagonal-z geometry. J. Nucl. Sci. Technol. 33 (8), 620–627.

Yamamoto, A., 2004. A simple and efficient control rod cusping model for three-dimensional pin-by-pin core calculation. Nucl. Technol. 145.